Effective field theory for Sp(N) antiferromagnets and their phase structure

Keisuke Kataoka, Shinya Hattori, and Ikuo Ichinose
Department of Applied Physics, Nagoya Institute of Technology, Nagoya, Japan
(Received 11 March 2010; revised manuscript received 13 April 2011; published 31 May 2011)

In this paper, we study quantum Sp(N) antiferromagnetic (AF) Heisenberg models by using the Schwinger-boson representation and the path-integral methods. We consider both the two-dimensional (2D) system at vanishing temperature and the 3D system at finite temperature (T). An effective field theory, which is an extension of the CP^{N-1} model in 3D, is derived and its phase structure is studied with the $1/N$ expansion. We also introduce a lattice gauge theoretical model of CP^{N-1} bosons, which is a counterpart of the effective field theory in the continuum, and study its phase structure by means of Monte Carlo simulations. For SU(N) AF magnets on the 2D square lattice, which is a specific case of the Sp(N) model, we introduce a spatial anisotropy in the exchange couplings and show that a phase transition from the ordered Néel state to the paramagnetic phase takes place as the anisotropy is increased. On the other hand for the 3D Sp(N) system at finite T, we clarify the global phase structure. As a parameter that controls explicit breaking of the SU(N) symmetry is increased, a new phase, which is similar to the spiral-spin phase in frustrated SU(2) spin systems, appears. It is shown that at that phase transition point, a local SU(2) gauge symmetry with composite SU(2) gauge field appears in the low-energy sector. This is another example of the symmetry-enhancement phenomenon at low energies. As it is expected that the Sp(4) AF magnets are realized by cold spin-3/2 fermions in an optical lattice, the above results might be verified by experiments in the near future.

DOI: 10.1103/PhysRevB.83.174449 PACS number(s): 75.50.Ee, 11.15.−q, 75.10.Jm

I. INTRODUCTION

The study of quantum antiferromagnets has been one of the most active areas in condensed matter physics. In particular, in the last decade, much attention has been paid to exotic phases and exotic phase transitions for which Landau's classic paradigm cannot be applicable.[1,2] It is expected that investigation of such exotic states is useful to understand anomalous properties of underdoped high-T_c materials.[3] Furthermore recent developments in technologies of ultracold atoms and optical lattice traps elevate purely academic quantum spin models to realistic ones, and these cold-atom systems are sometimes regarded as a final simulator for strongly correlated electron systems. Quantum SU(N) antiferromagnets are one of these examples. Theoretically these models can be studied by using the Schwinger-boson methods and the $1/N$ expansion.[4] In seminal papers,[5] it was shown that spin-$(N-1)/2$ (N is an even integer) cold-atom systems in an optical lattice with one atom per quantum well can be regarded as quantum Sp(N) antiferromagnets. There are two parameters J_1, J_2 in the Hamiltonian of the Sp(N) magnets and when $J_1 = J_2$, the symmetry is enhanced to SU(N) $\supset$ Sp(N) and an SU(N) quantum antiferromagnet is realized.

In the present paper, we shall study Sp(N) quantum antiferromagnets by using the slave-boson (Schwinger-boson) representation and the path-integral methods.[6] We first derive an effective field theory for the Sp(N) Heisenberg model. This field theory is an extension of the CP^{N-1} model for the SU(N) antiferromagnetic (AF) Heisenberg model. Then we investigate its phase structure by using the $1/N$ expansion. We also study numerically its lattice-gauge-model counterpart by means of Monte Carlo (MC) simulations.

This paper is organized as follows. In Sec. II, we shall derive the effective field theory for the Sp(N) AF Heisenberg model by using CP^{N-1} representation of (pseudo)spin degrees of freedom. We consider the 2-dimensional (2D) system at vanishing temperature (T) and also the 3-dimensional system at finite T, whose effective field theory is a gauge theory of CP^{N-1} bosons in 3D. In Sec. III, we study the effective field theory by the $1/N$ expansion. We focus on the quantum phase transition in the 2D system at $T = 0$ and the finite-T phase transition in the 3D system. We first show that in the SU(N) AF magnets with anisotropic exchange couplings on a square lattice, a quantum phase transition from the AF Néel state to the paramagnetic state takes place as the anisotropy is increased. This transition can be regarded also as a finite-T phase transition in the 3D system; i.e., the long-range AF order is destroyed by the thermal fluctuations. The above two states persist in the Sp(N) system in the vicinity of the SU(N) symmetric point $J_1 = J_2$. As J_2/J_1 is decreased to some critical value, a phase transition to a new phase with a composite vector-field condensation takes place and a new kind of spin order appears. In Sec. IV, we study a lattice version of the obtained field theory and show the results of the numerical study for the Sp(4) case. The obtained phase diagram is qualitatively in agreement with that obtained by the $1/N$ expansion, but we also find some discrepancy between the $1/N$ expansion and the numerical study, e.g., order of the phase transition, etc. Section V is devoted to our conclusions.

II. MODEL AND EFFECTIVE FIELD THEORY

A. Sp(N) Heisenberg model

In this paper, we shall study a system of fermions in 2D and 3D optical lattices. As we consider the case of *one atom at each well*, the quantum Hamiltonian of the system is given by Heisenberg models that describe dynamics of the spin degrees of freedom. Although the case of spin-3/2 fermions is the most realizable, we consider the general spin-$(N-1)/2$ (N is an even integer) cold atoms in the present paper. As in the usual spin-1/2 case, the exchange couplings are antiferromagnetic

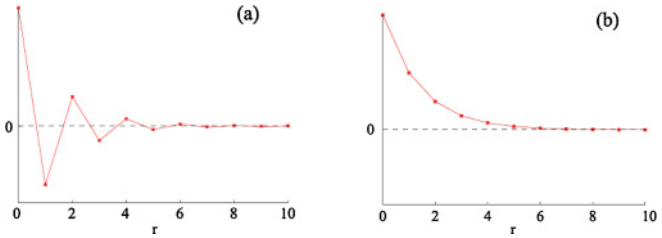

FIG. 1. (Color online) (a) Correlation of Γ^{ab}. (b) Correlation of Γ^{a}.

in these systems. The Hamiltonian of the Heisenberg model is given in terms of the spin operators $\vec{S}_i = (S_{i,x}, S_{i,y}, S_{i,z})$ at site i, which satisfy the usual commutation relations of the angular momentum. In previous papers,[5] it was shown that in the system of spin-3/2 fermions, the spin SU(2) symmetry is enlarged to Sp(4) symmetry as a result of the s-wave dominance of the scattering amplitude of fermions in a well. Therefore cold fermions in an optical lattice is an ideal system for study of the quantum Sp(N) AF magnets.

In this subsection, we consider the anisotropic Sp(N) Heisenberg model on a square lattice; i.e., exchange couplings in the x and y directions are different. Then the Hamiltonian is given as follows in the most general form with Sp(N) symmetry, which is a generalization of $\mathcal{H}_{\rm AF} = \sum J^{i,j} \vec{S}_i \cdot \vec{S}_j$,

$$\mathcal{H} = \sum_{\langle i,j \rangle} \left\{ J_1^{i,j} \sum_{a,b} \Gamma_i^{ab} \Gamma_j^{ab} - J_2^{i,j} \sum_{a} \Gamma_i^{a} \Gamma_j^{a} \right\}, \qquad (2.1)$$

where i, j denote lattice sites and $\Gamma^{ab} \in \mathbf{sp}(N)$ [the Lie algebra of Sp(N)] have $\frac{N(N+1)}{2}$ components. On the other hand, $\Gamma^{a} \in \mathbf{su}(N)/\mathbf{sp}(N)$, and there are $\frac{(N+1)(N-2)}{2}$ components. Hereafter in most cases, we consider the nearest-neighbor (NN) couplings and set the exchange couplings $J_1^{i,j}$ and $J_2^{i,j}$ as follows,

$$J_n^{i,i+\hat{x}} = J_{n,x},\ J_n^{i,i+\hat{y}} = J_{n,y}\ (n = 1,2),\ \text{otherwise } 0,$$

where $\hat{x}$ ($\hat{y}$) is the unit vector of the x (y) direction. For the $N = 4$ case,[7] the above generators are related to the (4×4)

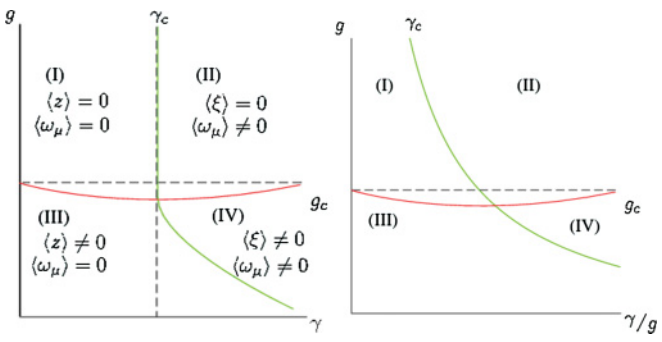

FIG. 2. (Color online) Phase diagram in γ-g and γ/g-g planes.

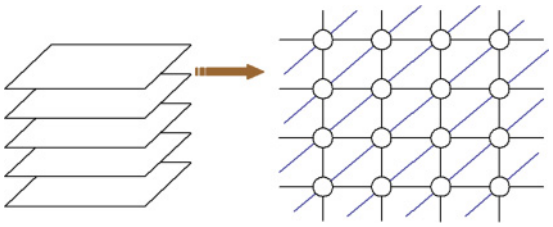

FIG. 3. (Color online) Lattice gauge model A_L in Eq. (5.1) is defined on layered triangular lattice.

spin matrices $\vec{S}$ as

$$\Gamma^1 = \frac{1}{\sqrt{3}}(S_x S_y + S_y S_x),\ \ \Gamma^2 = \frac{1}{\sqrt{3}}(S_z S_x + S_x S_z),$$
$$\Gamma^3 = \frac{1}{\sqrt{3}}(S_z S_y + S_y S_z),\ \ \Gamma^4 = \frac{1}{\sqrt{3}}\left(S_z^2 - \frac{5}{4}\right),\ \ (2.2)$$
$$\Gamma^5 = \frac{1}{\sqrt{3}}(S_x^2 - S_y^2),$$

and

$$\Gamma^{ab} = \frac{1}{2i}[\Gamma^a, \Gamma^b]. \qquad (2.3)$$

The Sp(4) case corresponds to the spin-3/2 system, and Γ^a involves even powers of the SU(2) spin matrices, whereas Γ^{ab} involves odd powers of the spin matrices. Then the long-range order of Γ^a indicates a spin-nematic order.

It is useful to introduce the matrix $\mathcal{J}$, which has the following properties and is a generalization of the time-reversal matrix $i\sigma^2$ in the SU(2) spin case,

$$\mathcal{J}^t = -\mathcal{J},\ \ \mathcal{J}^2 = -1,\ \ \mathcal{J}\Gamma^{ab}\mathcal{J} = (\Gamma^{ab})^t,\ \ \mathcal{J}\Gamma^{a}\mathcal{J} = -(\Gamma^{a})^t. \qquad (2.4)$$

To study the model (2.1) by means of field-theoretical methods, we introduce the Schwinger boson operator $\hat{b}_\alpha$ ($\alpha = 1, \ldots, N$) and represent the spin operators in the Hamiltonian (2.1) in terms of them, $\hat{\Gamma}_i^{ab} = \hat{b}_{i,\alpha}^\dagger \Gamma_{\alpha\beta}^{ab} \hat{b}_{i,\beta}$, $\hat{\Gamma}_i^{a} = \hat{b}_{i,\alpha}^\dagger \Gamma_{\alpha\beta}^{a} \hat{b}_{i,\beta}$. As in the spin-1/2 case, states in the Hilbert space of the Schwinger boson correspond to the states of spin-$(N-1)/2$ as

$$|S_z = (N-1)/2\rangle_S = \hat{b}_N^\dagger |0\rangle,\ \ldots, |S_z = -(N-1)/2\rangle_S = \hat{b}_1^\dagger |0\rangle, \qquad (2.5)$$

where $|0\rangle$ is the empty state of the Schwinger boson, whereas $|\cdot\rangle_S$ represents a state in the spin space. In terms of the Schwinger boson, the Hamiltonian $\mathcal{H}$ in Eq. (2.1) is rewritten as

$$\mathcal{H} = \sum_{\langle i,j \rangle} \left\{ 2\left(J_1^{i,j} - J_2^{i,j}\right) \hat{K}_{ij}^\dagger \hat{K}_{ij} - 2\left(J_1^{i,j} + J_2^{i,j}\right) \hat{Q}_{ij}^\dagger \hat{Q}_{ij} \right\}, \qquad (2.6)$$

where $\hat{Q}_{ij} = \mathcal{J}_{\alpha\beta} \hat{b}_{i,\alpha} \hat{b}_{j,\beta}$ and $\hat{K}_{ij} = \hat{b}_{\alpha,i}^\dagger \hat{b}_{\alpha,j}$. The operator $\mathcal{J}_{\alpha\beta} \hat{b}_{j,\beta}$ is the conjugate spinor of $\hat{b}_{j,\beta}$ and then $\hat{Q}_{ij}$ represents pairing of spins on the lattice sites i, j, whereas $\hat{K}_{ij}$ corresponds to the Schwinger boson (spinon) hopping. Both $\hat{Q}_{ij}$ and $\hat{K}_{ij}$ are invariant under Sp(N) transformations.

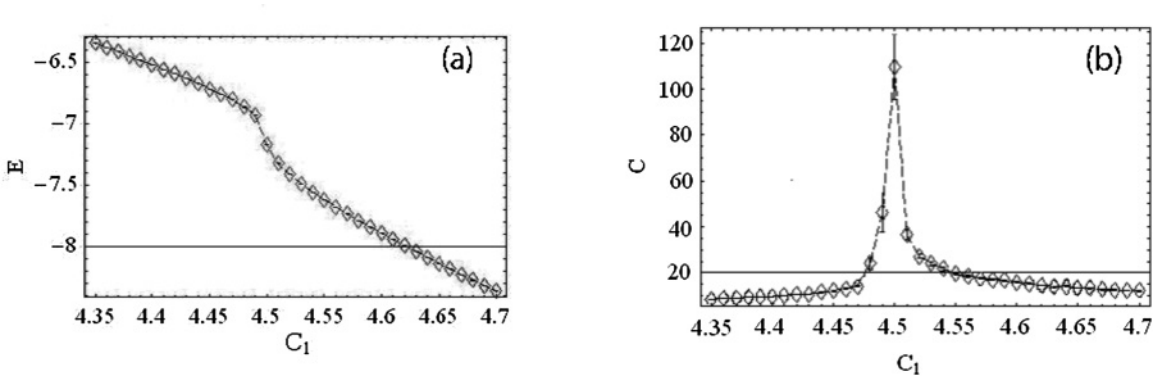

FIG. 4. (a) Energy E as a function of c_1 for $c_2 = c_3 = 0$. There exists a discontinuity at $c_1 = 4.5$. (b) Specific heat C as a function of c_1 for $c_2 = c_3 = 0$. There exists a sharp peak at $c_1 = 4.5$. System size $L = 20$.

As we are studying the system with one atom at each lattice site, we impose the following subsidiary condition,

$$\sum_{\alpha=1}^{N} \hat{b}^{\dagger}_{i,\alpha}\hat{b}_{i,\alpha}|\text{phys}\rangle = |\text{phys}\rangle, \tag{2.7}$$

as the physical-state condition. Then $\hat{\Gamma}^{a}_{i}$ form a vector representation of the Sp(N) group, whereas $\hat{\Gamma}^{ab}_{i}$ form an adjoint representation. Furthermore, $\hat{\Gamma}^{a}_{i}$ and $\hat{\Gamma}^{ab}_{i}$ together form a set of generators of the SU(N) Lie group. We redefine the exchange couplings as $J_{i,j} \equiv 2(J_1^{i,j} + J_2^{i,j})$, $J'_{i,j} \equiv 2(J_2^{i,j} - J_1^{i,j})$, then

$$\mathcal{H} = \sum_{\langle i,j\rangle}\{-J'_{i,j}\hat{K}^{\dagger}_{ij}\hat{K}_{ij} - J_{i,j}\hat{Q}^{\dagger}_{ij}\hat{Q}_{ij}\}. \tag{2.8}$$

From Eq. (2.8), it is obvious that when $J_{i,j} = 0$ ($J'_{i,j} = 0$), the model has the global SU(N) symmetry.[5] For the case $J_{i,j} = 0$, the spin at each site is in the fundamental representation of SU(N), whereas for the case $J'_{i,j} = 0$ spins on one sublattice are in the fundamental representation and those on the other sublattice are in the antifundamental representation of SU(N).

In the following subsections, we shall derive the effective field theory for the system (2.8) by using the path-integral methods.

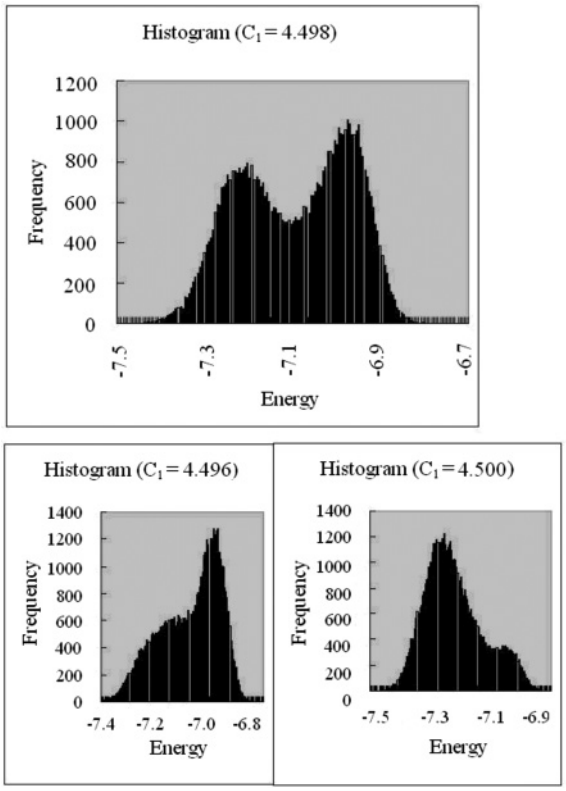

FIG. 5. Energy distribution $N[E]$ for the pure CP^3 model. At $c_1 = 4.498$, $N[E]$ has double-peak shape, whereas it has single peak at $c_1 = 4.496$ and 4.500. System size $L = 20$.

B. Effective field theory at $T = 0$

In this subsection, we shall derive the low-energy effective field theory of the Hamiltonian (2.8). To this end, we use the coherent path-integral methods. For the Schwinger boson, we use the CP^{N-1} boson that satisfies $\bar{z}_i \cdot z_i = \sum_\alpha \bar{z}_{i,\alpha} z_{i,\alpha} = 1$ corresponding to the condition (2.7). Then the partition function is given as

$$\begin{aligned} Z &= \int \mathcal{D}\bar{z}\mathcal{D}z\delta(\bar{z}\cdot z - 1)\exp\left[\int_0^\beta d\tau A(\tau)\right], \\ A(\tau) &= -\sum_{i,\alpha}\bar{z}_{i,\alpha}\dot{z}_{i,\alpha} - \mathcal{H}(z,\bar{z}), \end{aligned} \tag{2.9}$$

where $\beta = 1/(k_B T)$, $\dot{z}_i \equiv \frac{\partial z_i}{\partial \tau}$, and $\mathcal{H}(z,\bar{z})$ is obtained from Eq. (2.8) by replacing $\hat{b}_{i,\alpha} \to z_{i,\alpha}$ and $\hat{b}^{\dagger}_{i,\alpha} \to \bar{z}_{i,\alpha}$,

$$\mathcal{H}(z,\bar{z}) = \sum_{\langle i,j\rangle}\{-J'_{i,j}|\bar{z}_i z_j|^2 - J_{i,j}|z_i \mathcal{J} z_j|^2\}, \tag{2.10}$$

with $\bar{z}_i z_j = \sum_\alpha \bar{z}_{i,\alpha} z_{j,\alpha}$, etc. In order to derive the effective field theory from Eq. (2.9), we integrate out half of the CP^{N-1} variables, e.g., those at odd sites assuming a short-range AF order. Details of the calculation are similar to those of the SU(2) spin case given in Ref. 8. After the integration, we can consider a continuum limit of the effective model, as the remaining variables z_j at *even sites* can be regarded as a smoothly varying field $z(r)$ ($r_0 = \tau, r_1 = x, r_2 = y$). Hereafter

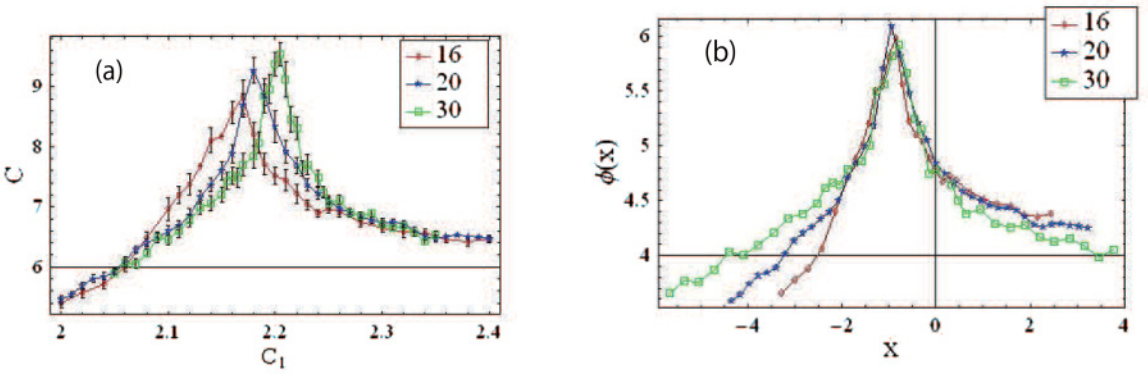

FIG. 6. (Color online) (a) C for $c_2 = 2.0$, $c_3 = 0$. System size is $L = 16, 20, 30$. (b) Scaling function $\phi(x)$ in finite-size scaling (5.4). Critical exponents and critical coupling are estimated as $\nu = 0.8$, $\sigma = 0.11$, and $c_{1c} = 2.23$.

we explicitly set the exchange couplings between adjacent spins as follows,

$$J_x = J_0, \quad J_y = \lambda J_0, \tag{2.11}$$

where λ is the parameter for the anisotropy between x and y directions. Then we obtain the action of the effective field theory for anisotropic SU(N) AF magnets in two dimensions at $T = 0$ as

$$S_0 = \frac{1}{2g}\int d^3r(\bar{D}_\mu \bar{z} D_\mu z + \sigma(|z|^2 - 1)), \tag{2.12}$$

where $D_\mu = \partial_\mu - \bar{z}\partial_\mu z$, and we have put the speed of light $c = \sqrt{2}(1+\lambda)J_0 a$ to unity. In S_0, σ is the Lagrange multiplier for the CP^{N-1} constraint, and the coupling constant g is given by

$$g = \frac{1+\lambda}{\sqrt{2\lambda}}a, \tag{2.13}$$

where a is the lattice spacing. From Eq. (2.13), it is obvious that the effective coupling g has the minimum at the isotropic point $\lambda = 1$. As we see in the following section, this means that the anisotropy tends to break the AF order of the ground state.

There also exists a Berry phase in the action,

$$S_B = -\frac{1}{6}\sqrt{\frac{2\lambda}{1+\lambda}}\int d^3r \epsilon_{\mu\nu\rho} D_\mu(\bar{D}_\nu \bar{z} D_\rho z). \tag{2.14}$$

The Berry phase (2.14) with the fractional coefficient depending on the anisotropy λ does not suppress effects of the instanton in contrast to that with an integer coefficient; i.e., S_B does not give any substantial effects on the phase structure and critical behavior.[9] For the case of the SU(2) AF magnets on a 2D lattice with anisotropic couplings, this observation has been verified directly by numerical study.[10]

C. Effective field theory for finite-T phase transition

In this subsection, we consider the quantum spin system (2.8) in a 3D cubic lattice, and focus on the isotropic NN coupling $J_{i,j} = J$, $J'_{i,j} = J'$. The effective field theory describing the finite-T phase transition of the system (2.8) is derived in the following way. In Eq. (2.9), we first ignore the time-derivative term $\bar{z}_i \dot{z}_i$ and then the partition function Z_{3D} is given as

$$Z_{3D} = \int \mathcal{D}\bar{z}\mathcal{D}z\delta(\bar{z}\cdot z - 1)\exp\left[-\beta\mathcal{H}_{3D}(z,\bar{z})\right], \tag{2.15}$$

where

$$\mathcal{H}_{3D}(z,\bar{z}) = \sum_{\langle i,j\rangle}\{-J'|\bar{z}_i z_j|^2 - J|z_i \mathcal{J} z_j|^2\}, \tag{2.16}$$

and i, j denote sites in the 3D cubic lattice. Due to the above approximation, numerical simulations of lattice CP^{N-1} boson model (2.15) become tractable as we see below.

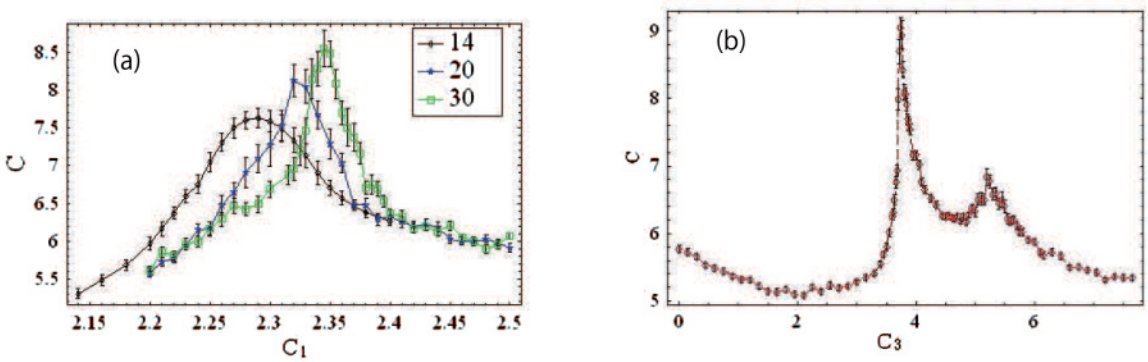

FIG. 7. (Color online) (a) C for $c_2 = 2.0$, $c_3 = 1.0$. System size is $L = 14, 20, 30$. Critical coupling is estimated as $c_1 = 2.35$. (b) C for $c_1 = 3.0$, $c_2 = 2.0$. System size is $L = 18$. There are two phase transitions at $c_3 = 3.7$ and 5.2.

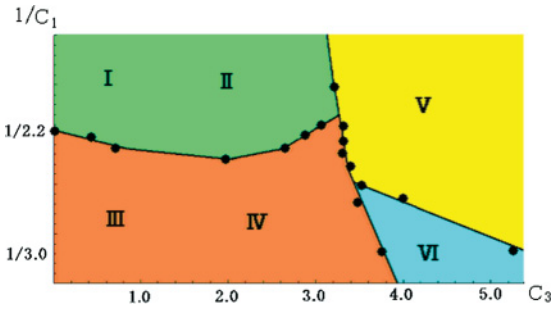

FIG. 8. (Color online) Phase diagram in $(c_3 - \frac{1}{c_1})$ plane for $c_2 = 2.0$. Solid lines are phase transition lines obtained by measurement of E and C. Dots denote phase transition points actually observed by measurement. Spin correlation functions exhibit different behavior in regions I–VI.

Physical meanings and the reliability of the approximation were discussed in detail in previous papers.[11]

To obtain the effective field theory for the lattice model (2.15), we first change variables as $z_i \to \mathcal{J}\bar{z}_i$ for $i \in$ odd site, and take a continuum limit by converting the difference on the lattice to a derivative in the continuum. Then we have

$$S_\gamma = \frac{1}{2g}\int d^3r(\bar{D}_\mu \bar{z} D_\mu z - \gamma(\bar{z}\mathcal{J}\bar{D}_\mu\bar{z})(z\mathcal{J}D_\mu z) + \sigma(|z|^2 - 1)), \tag{2.17}$$

where

$$\frac{1}{g} \sim \beta J/a, \quad \gamma = J'/J, \tag{2.18}$$

and μ in Eq. (2.17) denotes 3D spatial directions. It should be noted that S_γ in Eq. (2.17) reduces to S_0 in Eq. (2.12) for $\gamma = 0$. In the following sections, we shall study the field theory S_γ by means of both analytic and numerical methods.

III. PHASE STRUCTURE: ANALYTICAL STUDY

A. $1/N$ expansion: Case of small γ

The partition function of the effective field theory is given as

$$Z = \int \mathcal{D}z\mathcal{D}\bar{z}\mathcal{D}\sigma \exp\left(-\frac{N}{2g}\int d^3r[\bar{D}_\mu\bar{z}D_\mu z - \gamma(\bar{z}\mathcal{J}\bar{D}_\mu\bar{z})(z\mathcal{J}D_\mu z) + \sigma(|z|^2-1)]\right), \tag{3.1}$$

where we have introduced the factor N in front of the action to perform the $1/N$ expansion in the analytical study.[14] At $\gamma = 0$, the system (3.1) has the global SU(N) symmetry, $z(r) \to Vz(r)$, $V \in$ SU(N). We first consider the case of small γ, and put the following parameterization for z, $z = z_0 + u + iv$, where $z_0 = (n_0, 0, \ldots, 0)$, $u = (0, u_2, \ldots, u_N)$, and $v = (0, v_2, \ldots, v_N)$. The fields u and v are real vectors. Then from Eq. (3.1), effective action $S_{\rm eff}(n_0,\sigma)$ is obtained by integrating over u and v as

$$Z = \int \mathcal{D}n_0\mathcal{D}\sigma \exp[-S_{\rm eff}(n_0,\sigma)], \tag{3.2}$$

$$S_{\rm eff}(n_0,\sigma) = (N-1)\mathrm{Tr}\log\left(-\partial_\mu^2 + \sigma\right) + \frac{N}{2g}\int d^3x\sigma\left(n_0^2 - 1\right). \tag{3.3}$$

As the γ term generates only higher order terms of u and v, it does not give any effect in the leading order of $1/N$.

From $S_{\rm eff}(n_0,\sigma)$ in Eq. (3.3), gap equations are obtained as

$$\frac{\delta S_{\rm eff}(n_0,\sigma)}{\delta\sigma} = (N-1)\int\frac{d^3k}{(2\pi)^3}\frac{1}{k^2+\sigma} + \frac{N}{2g}(n_0^2 - 1) = 0, \tag{3.4}$$

$$\frac{\delta S_{\rm eff}(n_0,\sigma)}{\delta n_0} = \frac{N}{g}\sigma n_0 = 0. \tag{3.5}$$

We use the Pauli-Villars regularization with a cutoff Λ for the integral (3.4), and obtain the critical coupling g_c by putting $\sigma = n_0 = 0$,

$$\frac{1}{g_c} = \frac{\Lambda}{2\pi}, \tag{3.6}$$

where the cutoff Λ is related to the lattice spacing a of the original lattice as $\Lambda \sim \pi/a$. There are two phases, i.e., a strong-coupling phase for $g > g_c$,

$$\sqrt{\sigma_0} = \frac{2\pi}{N}\left(\frac{1}{g_c} - \frac{1}{g}\right), \quad n_0 = 0, \quad \sigma_0 = \langle\sigma\rangle, \tag{3.7}$$

and a weak-coupling phase for $g < g_c$,

$$n_0^2 = 1 - \frac{g}{g_c}, \quad \sigma_0 = 0. \tag{3.8}$$

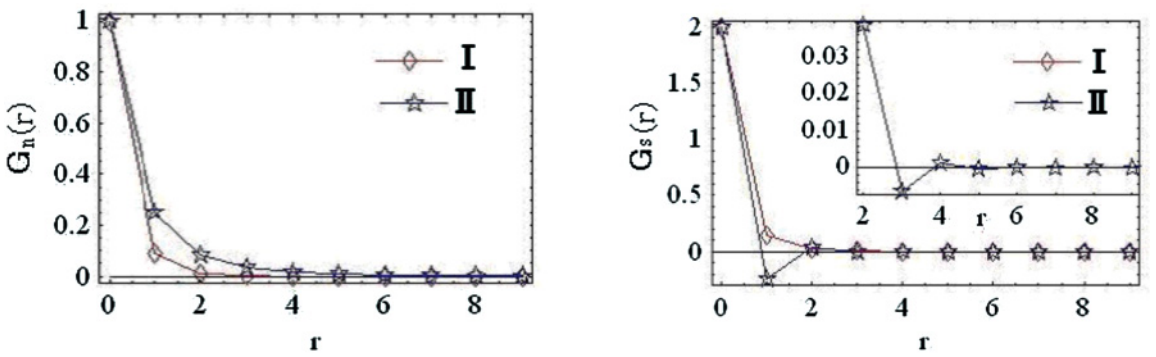

FIG. 9. (Color online) Spin correlation functions in I and II in phase diagram Fig. 8. Both $G_n(r)$ and $G_s(r)$ have no long-range order in I and II; however in II $G_s(r)$ exhibits a short-range spiral order.

For $g < g_c$, Sp(N) symmetry is spontaneously broken and both spins Γ^{ab} and Γ^a have long-range order. In a later section, the above result will be verified by the numerical study of the lattice model for the effective field theory.

The existence of the critical coupling g_c indicates that at $T = 0$ there is a critical anisotropic parameter λ_c for the SU(N) AF magnets in the square lattice, beyond which AF long-range order disappears.[12] On the other hand for the 3D AF magnets at finite T, there exists a critical temperature $T_c \sim Jg_c/a$, below which the AF long-range order exists.

B. Case $\gamma \approx 1$: Auxiliary fields

In this subsection, we shall consider the case $\gamma \approx 1$. It is useful to introduce two kinds of auxiliary vector fields λ_μ and ω_μ to investigate the phase structure of the model. The partition function in (3.1) is rewritten as

$$Z = \int \mathcal{D}z\mathcal{D}\bar{z}\mathcal{D}\sigma\mathcal{D}\lambda_\mu\mathcal{D}\bar{\omega}_\mu\mathcal{D}\omega_\mu \exp\left(-\frac{N}{2g}\int d^3r\ \mathcal{L}\right) \tag{3.9}$$

where

$$\mathcal{L} = \bar{z}\big(-\partial_\mu^2 + i\lambda_\mu \overset{\leftrightarrow}{\partial}_\mu + \lambda_\mu^2 + \gamma|\omega_\mu|^2 + \sigma\big)z - z(\gamma\bar{\omega}_\mu\mathcal{J}\partial_\mu)z - \bar{z}(\gamma\omega_\mu\mathcal{J}\partial_\mu)\bar{z} - \sigma, \tag{3.10}$$

with

$$\bar{z}\lambda_\mu \overset{\leftrightarrow}{\partial}_\mu z = \lambda_\mu(\bar{z}\cdot\partial_\mu z - \partial_\mu\bar{z}\cdot z).$$

1. Strong-coupling region

First we shall study the model (3.9) in the strong-coupling region $g > g_c$, in which $n_0 = 0$, $\langle\sigma\rangle > 0$. In particular, we are interested in the possibility of the condensation of ω_μ. As the Lagrangian $\mathcal{L}$ in Eq. (3.10) is a quadratic form of z, integration over z can be done. For smoothly varying configurations of ω_μ, the effective action is obtained as

$$N\int\frac{d^3p}{(2\pi)^3}\bar{\omega}_\mu(p)\Big[\frac{\gamma^2}{16\pi\sqrt{\sigma}}(p^2\delta_{\mu\nu} - p_\mu p_\nu) + \gamma(1-\gamma)\Omega\delta_{\mu\nu}\Big]\omega_\nu(p), \tag{3.11}$$

where $\omega_\mu(p)$ is the Fourier-transformed field of ω_μ and Ω is a constant. From Eq. (3.11), it is obvious that ω_μ behaves like a massive vector field for $\gamma < 1$, for $\gamma = 1$ it becomes massless and behaves like a kind of gauge field, and finally for $\gamma > 1$ its nonvanishing condensation is expected to occur. More detailed study on the case $\gamma = 1$ will be given in a later section, and it is shown there that an SU(2) gauge model really appears.

Let us study the case $\gamma > 1$ somewhat in detail in the large-N limit. Condensation of ω_μ apparently breaks the rotational symmetry of the space (or $\frac{\pi}{2}$-rotation of the square lattice) and also the U(1) gauge symmetry to Z_2.[2,15] Here we assume $\langle\omega_\mu\rangle = \omega\delta_{\mu x}(\omega \neq 0)$ without loss of generality.[16] We also assume that ω is real by the gauge symmetry of the system. Then in the phase with condensation of ω_x, the action of $z(r)$ is given as follows from (3.10):

$$S_z = \frac{N}{2g}\int d^3r\big[-\bar{z}\partial_\mu^2 z - \gamma\omega(z\mathcal{J}\partial_x z) - \gamma\omega(\bar{z}\mathcal{J}\partial_x\bar{z}) + \sigma(|z|^2 - 1)\big], \tag{3.12}$$

and it can be diagonalized by introducing field $\xi(r)$ as

$$z(r) = \frac{1}{\sqrt{2}}\{e^{-i\gamma\omega x}\xi(r) + e^{i\gamma\omega x}[i\mathcal{J}\bar{\xi}(r)]\}, \tag{3.13}$$

$$S_\xi = S_z = \frac{N}{2g}\int d^3r\big\{\bar{\xi}\big(-\partial_\mu^2 + \gamma(1-\gamma)\omega^2\big)\xi + \sigma(\bar{\xi}\xi - 1)\big\}. \tag{3.14}$$

From Eq. (3.14), it is obvious that the field $\xi(r)$ acquires its mass squared $\sigma' = \sigma + \gamma(1-\gamma)\omega^2$.

From S_ξ in Eq. (3.14), we can derive a gap equation and determine the critical coupling g_c as in the previous case,

$$\sqrt{\sigma'} = 2\pi\left(\frac{1}{g_c} - \frac{1}{g}\right), \tag{3.15}$$

$$\frac{1}{g_c} = \frac{\Lambda}{2\pi}. \tag{3.16}$$

The above critical value g_c is the same with that obtained for the case of small γ.

In the large-N limit, spin correlations are obtained from Eq. (3.13) for $g > g_c$, see Fig. 1.

2. Weak-coupling region

Finally we shall consider the weak-coupling region $g < g_c$, in which the condensation of $z(r)$ occurs. As in the strong-coupling region discussed in the previous subsection, we expect the condensation of ω_μ for large γ. However as the condensation of $z(r)$ gives an effective mass for ω_μ by the Anderson-Higgs mechanism [see Eq. (3.10)], the critical value γ_c is $\gamma_c > 1$. The value of γ_c can be estimated by detailed calculation.

For $\gamma > \gamma_c$, the dynamics of $z(r)$ is described by S_z in Eq. (3.14). Effective coupling g_c for the condensation of $z(r)$ and $\xi(r)$ is estimated as before and the same result is obtained with (3.16). For $g < g_c$ and $\gamma > \gamma_c$, $\xi(r)$ condenses and nontrivial correlations of the spin operators $\hat{\Gamma}^{ab}$ appear as a result of $\langle\omega_\mu\rangle \neq 0$. In this phase,

$$\langle\hat{\Gamma}^{ab}(r)\rangle = \langle\bar{z}(r)\Gamma^{ab}z(r)\rangle = n_1^{ab}\cos(2\gamma\omega x) + n_2^{ab}\sin(2\gamma\omega x), \tag{3.17}$$

where $n_1^{ab} = \mathrm{Re}[\langle\xi\rangle\mathcal{J}\Gamma^{ab}\langle\xi\rangle]$, $n_2^{ab} = \mathrm{Im}[\langle\xi\rangle\mathcal{J}\Gamma^{ab}\langle\xi\rangle]$. On the other hand, $\langle\hat{\Gamma}^a(r)\rangle = \langle\bar{\xi}\rangle\Gamma^a\langle\xi\rangle$. Therefore $\langle\hat{\Gamma}^{ab}(r)\rangle$ exhibits the spiral order, whereas $\langle\hat{\Gamma}^a(r)\rangle$ exhibits the ordinary long-range order.

IV. SU(2) GAUGE THEORY AT $\gamma = 1$

In the previous section, we found that the composite vector field ω_μ behaves like a massless gauge field at $\gamma = 1$, and for $g < g_c$ it acquires mass squared proportional to $\langle\bar{z}\cdot z\rangle$ as a result of the Anderson-Higgs mechanism. In this section, we shall explicitly show that the three real vector fields

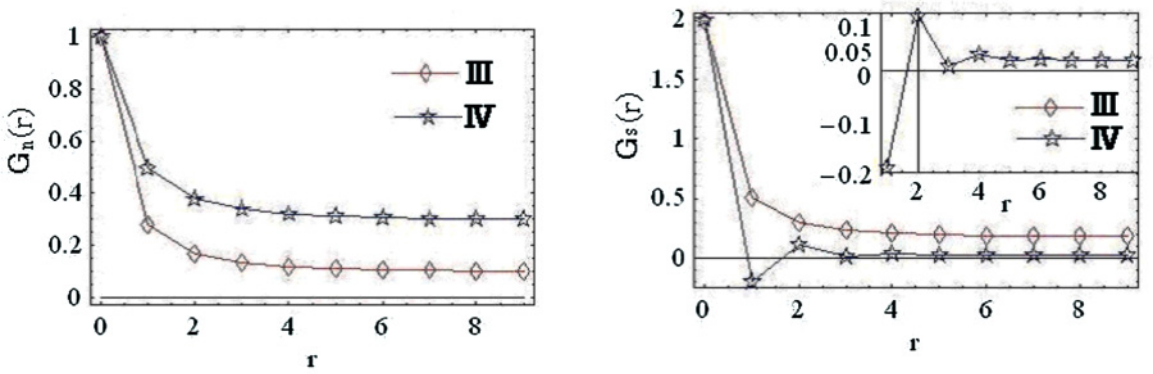

FIG. 10. (Color online) Spin correlation functions in III and IV in phase diagram Fig. 8. $G_n(r)$ has long-range order in both III and IV. In IV, $G_s(r)$ exhibits a long-range spiral order, whereas it has the usual long-range order in III.

$(\lambda_\mu, \omega_\mu^R, \omega_\mu^I)$ form an SU(2) gauge field minimally coupled with z at $\gamma = 1$, where $\omega_\mu = \omega_\mu^R + i\omega_\mu^I$. This is another example of the symmetry-enhancement phenomenon, i.e., an emergent symmetry at low energies.

We start with the action $\mathcal{L}_{\gamma=1}$ in Eq. (3.10),

$$\mathcal{L}_{\gamma=1} = \bar{z}\big(-\partial_\mu^2 + i\lambda_\mu \overset{\leftrightarrow}{\partial}_\mu + \lambda_\mu^2 + |\omega_\mu|^2 + \sigma\big)z - z(\bar{\omega}_\mu \mathcal{J}\partial_\mu)z - \bar{z}(\omega_\mu \mathcal{J}\partial_\mu)\bar{z} - \sigma, \tag{4.1}$$

where we have put $\gamma = 1$. Hereafter we explicitly consider the CP^3 case but generalization to an arbitrary N is straightforward. We first redefine the CP^3 field $Z(r)$ from the original $z(r)$ as $Z(r) = (z_1(r), z_2(r), \bar{z}_4(r), -\bar{z}_3(r))^t$. It is easily verified that $Z(r)$ is a CP^3 field; i.e., $\sum_{i=1}^4 |Z_i(r)|^2 = 1$.

It is straightforward to verify the following equation,

$$\bar{z} \overset{\leftrightarrow}{\partial}_\mu z = \bar{Z}\Sigma_3 \overset{\leftrightarrow}{\partial}_\mu Z, \tag{4.2}$$

where

$$\Sigma_3 = \begin{pmatrix} 1 & 0 & 0 & 0 \\ 0 & 1 & 0 & 0 \\ 0 & 0 & -1 & 0 \\ 0 & 0 & 0 & -1 \end{pmatrix}. \tag{4.3}$$

Similarly

$$\bar{\omega}_\mu(z\mathcal{J}\partial_\mu)z + \omega_\mu(\bar{z}\mathcal{J}\partial_\mu)\bar{z} = i\omega_\mu^R(\bar{Z}\Sigma_2 \overset{\leftrightarrow}{\partial}_\mu Z) + i\omega_\mu^I(\bar{Z}\Sigma_1 \overset{\leftrightarrow}{\partial}_\mu Z), \tag{4.4}$$

where

$$\mathcal{J} = \begin{pmatrix} 0 & 0 & 0 & 1 \\ 0 & 0 & -1 & 0 \\ 0 & 1 & 0 & 0 \\ -1 & 0 & 0 & 0 \end{pmatrix}, \quad \Sigma_2 = \begin{pmatrix} 0 & 0 & i & 0 \\ 0 & 0 & 0 & i \\ -i & 0 & 0 & 0 \\ 0 & -i & 0 & 0 \end{pmatrix},$$

$$\Sigma_1 = \begin{pmatrix} 0 & 0 & 1 & 0 \\ 0 & 0 & 0 & 1 \\ 1 & 0 & 0 & 0 \\ 0 & 1 & 0 & 0 \end{pmatrix}. \tag{4.5}$$

It is obvious that $\Sigma_i (i = 1,2,3)$ satisfy the SU(2) algebra. Let us define the SU(2) gauge field $\vec{\mathcal{A}}_\mu$ as $\vec{\mathcal{A}}_\mu = (\omega_\mu^I, \omega_\mu^R, \lambda_\mu)$, then the Lagrangian (4.1) can be rewritten as follows,

$$\mathcal{L}_{\gamma=1} = |(\partial_\mu + i\vec{\Sigma}\cdot\vec{\mathcal{A}}_\mu)Z|^2 + \sigma|Z|^2 - \sigma. \tag{4.6}$$

The lattice gauge model corresponding to the above SU(2) gauge theory (4.6) is under study and the result will be reported in a future publication. However phase structure of the system can be inferred by qualitative discussion. As in the usual CP^{N-1} model coupled with the U(1) gauge field, there exists a phase transition that separates ordered and disordered phases. However, as the SU(2) gauge field fluctuates the hopping of the spinon $Z(r)$ more strongly than the U(1) gauge field, the critical coupling $g_c(\gamma = 1)$ is expected to be smaller than $g_c(\gamma = 0)$. From this consideration, we expect that the critical coupling $g_c(\gamma)$ is a decreasing function of γ for $\gamma < \gamma_c$, although in the previous discussion for small $\gamma \ll 1$ by the

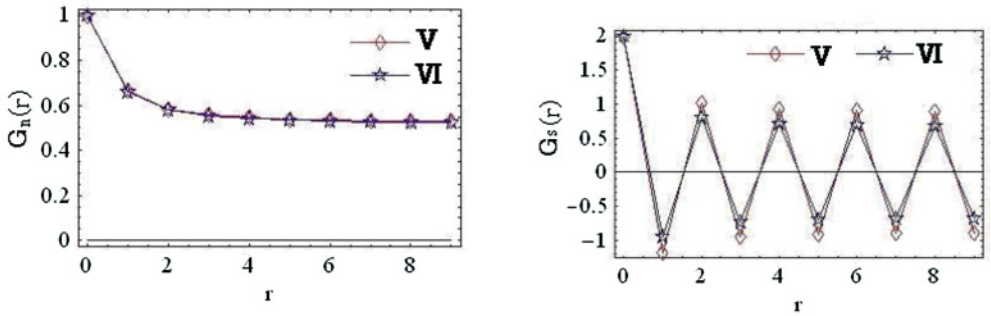

FIG. 11. (Color online) Spin correlation functions in V and VI in phase diagram Fig. 8. Both $G_n(r)$ and $G_s(r)$ exhibit the same behavior in V and VI.

$1/N$ expansion we did not find any γ dependence of g_c. As γ exceeds γ_c, the condensation of ω_μ tends to occur and fluctuations of ω_μ are suppressed. Moreover the original U(1) gauge symmetry reduces to Z_2 gauge symmetry by the Anderson-Higgs mechanism and fluctuations of λ_μ are also suppressed. Then $g_c(\gamma)$ starts to increase at $\gamma = \gamma_c$. The above expectation will be confirmed by the numerical study of the lattice-gauge model in the following section. The expected phase diagram is shown in the γ-g plane in Fig. 2.

In the following section, we shall introduce a lattice model for the effective field theory with a general value of γ, and study it by means of MC simulations.

V. NUMERICAL STUDY

A. Lattice CP[3] model

In this section we formulate the effective field theory (3.1) on a 3D lattice and investigate its phase structure by means of numerical methods. If one tries to perform numerical studies of the original system Eq. (2.9) directly by means of the MC simulations, one immediately encounters difficulty in the importance-sampling procedure, since the first term of $A(\tau)$, $\bar{z}_i \partial_\tau z_i$, is purely imaginary. In Sec. II B, we derived the effective field theory by analytically integrating out CP^{N-1} variables at all odd sites. As a result, the derived field-theory model has the real-valued action Eq. (2.12).[17] On the other hand in Sec. II C, we considered the 3D system at finite T and derived the effective field theory that describes finite-T phase transitions.

In the present section, we explicitly consider the Sp(4) model whose action A_L is given as follows:

$$\begin{aligned} A_L = {} & c_1 \sum_{r,\mu} \bar{z}_{r+\mu} U_{r\mu} z_r + \text{c.c.} \\ & + c_2 \sum_{r,\mu,\nu} U_{r\mu} U_{r+\mu,\nu} \bar{U}_{r+\nu,\mu} \bar{U}_{r\nu} + \text{c.c.} \\ & + c_3 \sum_{r,\mu} |z_r \mathcal{J} z_{r+\mu}|^2 + c_4 \sum_r |z_r \mathcal{J} z_{r+1+2}|^2, \end{aligned} \tag{5.1}$$

where r denotes the cubic lattice site; $\mu = (1,2,3)$ is the direction index and it also denotes the unit vector in the μ direction. Field z_r are CP^3 variables and $U_{r\mu}$ is a U(1) gauge field defined on link (r,μ), $U_{r\mu} \sim e^{i\lambda_\mu(r)}$. The parameters $c_1 \propto a/g$, $c_3 \propto \gamma/g$, and the c_2 term is the lattice Maxwell term (the so-called Wilson term) corresponding to $(\partial_\mu A_\nu - \partial_\nu A_\mu)^2$ in the continuum space-time.[18] We have also added the c_4 term on the diagonal lines in the 2D layers that correspond to the exchange couplings between spins like $\hat{Q}^\dagger_{i,i+1+2} \hat{Q}_{i,i+1+2}$. Therefore, the model A_L is defined on the *layered triangular lattice*. See Fig. 3.

The partition function Z_L is given as follows:

$$Z_L = \int [DU][Dz D\bar{z}]_{\mathrm{CP}}\, e^{A_L}, \tag{5.2}$$

where $[Dz D\bar{z}]_{\mathrm{CP}}$ denotes the integration over CP^3 variables. As A_L is real and has the lower bound, the MC simulations for Eq. (5.2) can be performed without any difficulty.

For the MC simulations, we used the standard Metropolis algorithm of local update. The typical statistics was 10^5 MC steps per sample, and the averages and errors were estimated over ten samples. The typical acceptance ratio was about 50%. We also used multihistogram methods to obtain reliable results near the phase transition point.[19]

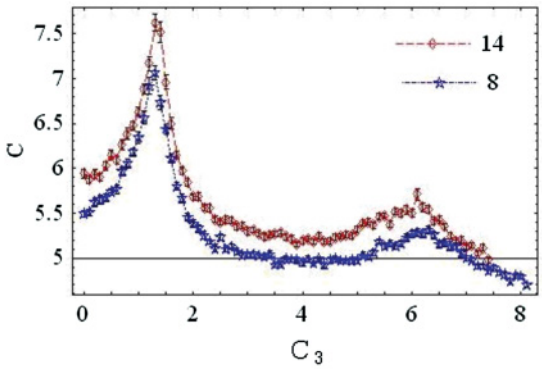

FIG. 12. (Color online) Specific heat on line $c_3 = c_4$ with $c_1 = 6$, $c_2 = 0$. Result indicates two phase transitions on the line. $L = 8$ and 14.

B. Case of $c_3 = c_4 = 0$

We first consider the case of the pure CP^3 model with $c_2 = c_3 = c_4 = 0$, which corresponds to the anisotropic SU(4) AF magnet.[13] We calculate the internal energy $E = \langle A_L \rangle / L^3$ and the specific heat $C = \langle (A_L - E)^2 \rangle / L^3$ to study phase structure, where L^3 is the lattice size and we impose the periodic boundary condition in most of calculations. In Fig. 4, we show E and C as a function of c_1. It is obvious that E has a discontinuity at $c_1 \simeq 4.5$ and C has a very large peak at $c_1 \simeq 4.5$, which indicates a first-order phase transition. In order to verify this observation, we calculated density of states $N[E]$ that is defined as

$$N[E] = \int [DU][Dz D\bar{z}]_{\mathrm{CP}}\, \delta(A_L - E)\, e^{A_L}. \tag{5.3}$$

The result in Fig. 5 shows that $N[E]$ has a double-peak shape at $c_1 = 4.498$, whereas it has a single peak at the other couplings. This confirms the existence of the first-order phase transition in the CP^3 model, although the corresponding phase transitions in the CP^1 and CP^2 models are of second order. Study of the correlation functions of the spin operators given later on verifies that the phase transition from Néel to paramagnetic states takes place at $c_1 = 4.498$.

The CP^{N-1} model in 3D space-time was studied with the $1/N$ expansion and it was suggested that there existed a second-order phase transition from ordered to disordered phases as the coupling constant is increased. However the present investigation by means of the MC simulations shows that the order of the phase transition varies as a function of the parameter N. A similar phenomenon was recently observed with some related models, e.g., the multi-Higgs U(1) gauge model in 3D.[20] We also studied finite but small c_2 cases and found that the phase transition is still of first order. However at an intermediate value of c_2, C exhibits the finite-size scaling (see Fig. 6); i.e., the data of $C(c_1, L)$ for system size L and $c_2 = 2.0$ can be fitted as follows with a scaling function $\phi(x)$:[21]

$$C(c_1, L) = L^{\sigma/\nu} \phi(L^{1/\nu} \epsilon), \quad \epsilon = (c_1 - c_{1c})/c_{1c}, \tag{5.4}$$

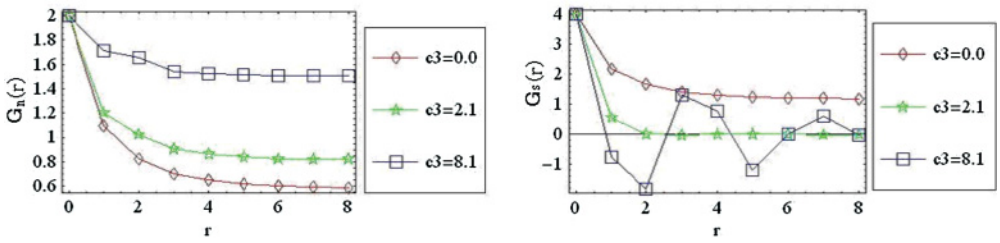

FIG. 13. (Color online) Spin correlation functions for $c_1 = 6.0$ and $c_2 = 0$.

where c_{1c} is the critical coupling at infinite system size and estimated as $c_{1c} = 2.23$. This fact means that the phase transition becomes of second order as the value of c_2 is increased.

C. Effect of c_3 term and phase diagram

Let us turn on the c_3 term and see how the location of the phase transition varies. We studied the system by varying the value of c_1 with fixed c_3 and found a clear signal of phase transitions; see, e.g., C for $c_2 = 2.0$, $c_3 = 1.0$ in Fig. 7(a). We also investigated the phase structure of the system with c_1 fixed and c_3 varied, and found that there is another phase transition line. See Fig. 7(b).

The obtained phase diagram in the $(c_3 - \frac{1}{c_1})$ plane is shown in Fig. 8. There are four phases, which are identified by the measurement of E and C. We also investigated the behavior of the correlation function of the spin operators,

$$G_n(r) = \sum_a \left\langle \Gamma^a_{r'+r} \Gamma^a_{r'} \right\rangle, \quad G_s(r) = \sum_{a,b} \left\langle \Gamma^{ab}_{r'+r} \Gamma^{ab}_{r'} \right\rangle. \quad (5.5)$$

As we expected that a phase transition to a spiral state would take place as the parameters were increased, we took the free boundary condition in the two spatial directions. We found that the correlators exhibit different behavior in the six regions I–VI shown in Fig. 8. It is obvious that not only simple AF correlations but also ferromagnetic (FM) correlations appear in these correlators. For example, in the regions I and II (III and IV), the correlation of the nematic order $G_n(r)$ exhibits the same behavior, but the spin correlator $G_s(r)$ behaves differently in I and II (III and IV), see Fig. 9 (Fig. 10). We have observed no phase boundary between the I and II (III and IV) regions on which the internal energy E and specific heat C exhibit anomalous behavior. However, from the result of the spin correlation function $G_s(r)$, we expect that the phases $\langle \omega_\mu \rangle \neq 0$, $\langle \xi(r) \rangle = 0$ and $\langle \omega_\mu \rangle \neq 0$, $\langle \xi(r) \rangle \neq 0$ are realized in the regions II and IV, respectively. On the other hand, there are no phases in the effective field theory that correspond to phases V and VI (Fig. 11) of the FM long-range order in the lattice model. This result is plausible because the effective field theory in the continuum space(-time) has been derived by assuming smooth configurations of z_i having short-range AF order, and therefore it cannot describe the phase with the FM order.

D. Effect of c_4 term

Finally we turn on the c_4 term in addition to the c_3 term. Numerical study of the system was performed along the line $c_3 = c_4$ with $c_1 = 6.0$ and $c_2 = 0$ in the phase diagram. The observed C as a function of $c_3 = c_4$ is shown in Fig. 12. There are two phase transitions, one at $c_3 = c_4 \simeq 0.7$ and the other at $c_3 = c_4 \simeq 6.0$. In order to understand these phase transitions, we calculated the spin correlation functions in each phase, which are shown in Fig. 13. From the result, it is obvious that the AF order disappears first and then at the second transition the spiral state appears. This state corresponds to the state with nonvanishing $\langle \xi(r) \rangle \neq 0$ studied in the previous sections. Some related models of Sp(N) spins on an anisotropic triangular lattice were studied in the large-N limit, and a phase with an incommensurate spin order, similar to the above, was found.[22]

VI. CONCLUSION

In the present paper, we have studied the Sp(N) AF Heisenberg models that are expected to be realized in cold-atom systems in an optical lattice. We first focused on the ground-state structure of the system in 2D and derived the effective field theory for the system. Then we considered finite-T properties of the Sp(N) AF Heisenberg magnets in 3D and derived the effective field theory, which is a kind of extension of the CP^{N-1} nonlinear σ model. We studied the phase structure and critical behavior of the effective field theory by using the $1/N$ expansion. We found that the spatial anisotropy induces a phase transition from the ordered state to the paramagnetic state. As the explicit breaking of the SU(N) symmetry increases, the system exhibits a spiral order of the adjoint representation of the Sp(N) group. This state also has a nematic order of vector representation of the Sp(N) group.

We also introduced a lattice gauge-model counterpart of the effective field theory and studied its phase structure by means of the MC simulations. We found a similar phase diagram to that of the field theory, but the order of the phase transitions is different in the two systems.

In Ref. 23, a finite-temperature phase diagram of the Sp(N) model was studied by using Ginzburg-Landau theory in terms of gauge-invariant spin fields, $\phi^{ab} = z^\dagger \Gamma^{ab} z$, $\phi^a = z^\dagger \Gamma^{ab} z$. There the quantum phase transition of the Sp(4) spin system in a 3D stacked square lattice was also discussed. The phase transition from the CP^3 Néel ordered state to the photon liquid state was predicted. In the present study, the (3+1)D counterpart of the lattice model (5.1) describes the quantum phase transition of the Sp(4) spin system in a 3D stacked square lattice. It is expected that a deconfined photon phase exists for sufficiently large c_2. In fact, the U(1) gauge theory of the CP^1 field in (3+1)D was studied previously,[24] and it was found

that the phase transition from the CP[1] Néel ordered state to the photon liquid state actually takes place and is of second order.

It is interesting to study the effects of hole doping on the Sp(N) AF magnets and investigate how the long-range orders are broken and whether a new phase with hole-pair condensation appears. This system is an extension of the t-J model for high-temperature superconductivity. This problem is under study and we hope to report the results in a future publication.

ACKNOWLEDGMENTS

This work was partially supported by a Grant-in-Aid for Scientific Research from the Japan Society for the Promotion of Science under Grant No. 20540264.

[1]T. Senthil, L. Balents, S. Sachdev, A. Vishwanath, and M. P. A. Fisher, Phys. Rev. B **70**, 144407 (2004); T. Senthil, A. Vishwanath, L. Balents, S. Sachdev, and M. P. A. Fisher, Science **303**, 1490 (2004).

[2]S. Sachdev, Nature Phys. **4**, 173 (2008).

[3]A. P. Lee, N. Nagaosa, and X.-G. Wen, Rev. Mod. Phys. **78**, 17 (2006).

[4]N. Read and S. Sachdev, Nucl. Phys. B **316**, 609 (1989); Phys. Rev. B **42**, 4568 (1990).

[5]C. Wu, J. P. Hu, and S. C. Zhang, Phys. Rev. Lett. **91**, 186402 (2003); C. Wu, Mod. Phys. Lett. B **20**, 1707 (2006).

[6]For recent studies of Sp(N) spin models, see for example, D. Schuricht and S. Rachel, Phys. Rev. B **78**, 014430 (2008); R. Flint, M. Dzero, and P. Coleman, Nature Phys. **4**, 643 (2008); R. Flint and P. Coleman, Phys. Rev. B **79**, 014424 (2009).

[7]Y. Qi and C. Xu, Phys. Rev. B **78**, 014410 (2008).

[8]I. Ichinose and T. Matsui, Phys. Rev. B **45**, 9976 (1992); H. Yamamoto, G. Tatara, I. Ichinose, and T. Matsui, *ibid*. **44**, 7654 (1991).

[9]D. Yoshioka, G. Arakawa, I. Ichinose, and T. Matsui, Phys. Rev. B **70**, 174407 (2004).

[10]S. Wenzel and W. Janke, Phys. Rev. B **79**, 014410 (2009).

[11]K. Nakane, T. Kamijo, and I. Ichinose, Phys. Rev. B **83**, 054414 (2011); A. Shimizu, K. Aoki, K. Sakakibara, I. Ichinose, and T. Matsui, *ibid*. **83**, 064502 (2011).

[12]For the SU(N) ($N \leqslant 4$) Heisenberg model with isotropic nearest-neigbhor coupling J and vanishing $J' = 0$, it is known that the ground state has AF long-range order.[13] This means that effective coupling of these spin models is smaller than the critical coupling g_c.

[13]K. Harada, N. Kawashima, and M. Troyer, Phys. Rev. Lett. **90**, 117203 (2003); for study on SU(4) Heisenberg models with $J = 0$, $J' \neq 0$, see Y. Q. Li, M. Ma, D. N. Shi, and F. C. Zhang, *ibid.* **81**, 3527 (1998).

[14]I. Ya. Aref'eva and S. I. Azakov, Nucl. Phys. B **162**, 298 (1980).

[15]K. Nakane, A. Shimizu, and I. Ichinose, Phys. Rev. B **80**, 224425 (2009).

[16]Although it seems plausible to put $\langle \omega_\mu \rangle =$ constant in the effective field theory, this corresponds to the assumption that $\langle z_{e'} \mathcal{J} z_e \rangle =$ constant for all the NN even-site pairs e and e' on the original 2D lattice.

[17]This situation is similar to the momentum integration in the imaginary-time formalism of point-particle quantum mechanics,

$$\int [dp]\, e^{\int d\tau (ip\dot{q} - \frac{p^2}{2m})} = e^{-\int d\tau \, \frac{m}{2}\dot{q}^2}.$$

[18]Here we should notice that the lattice gauge model A_L is a compact U(1) gauge model as the original Sp(N) spin model with the Schwinger-boson representation has the compact U(1) gauge symmetry.

[19]A. M. Ferrenberg and R. H. Swendsen, Phys. Rev. Lett. **63**, 1195 (1989).

[20]T. Ono, S. Doi, Y. Hori, I. Ichinose, and T. Matsui, Ann. Phys. (N.Y.) **324**, 2453 (2009); for quantum SU(N) Heisenberg model, K. S. D. Beach, F. Alet, M. Mambrini, and S. Capponi, Phys. Rev. B **80**, 184401 (2009).

[21]See for example, J. M. Thijissen, *Computational Physics* (Cambridge University Press, Cambridge, 1999).

[22]C. H. Chung and J. B. Marston, J. Phys. Condens. Matter **13**, 5159 (2001).

[23]C. Xu, Phys. Rev. B **80**, 184407 (2009).

[24]K. Sawamura, T. Hiramatsu, K. Ozaki, I. Ichinose, and T. Matsui, Phys. Rev. B **77**, 224404 (2008).